Lawrence Berkeley National Laboratory
Recent Work

Title
In-situ, microscale characterization of heterogeneous deformation around notch in martensitic Shape Memory Alloy

Permalink
https://escholarship.org/uc/item/8zk17809

Authors
Paul, PP
Paranjape, HM
Tamura, N
et al.

Publication Date
2020-01-13

DOI
10.1016/j.msea.2019.138605

Peer reviewed

eScholarship.org Powered by the California Digital Library
University of California

ResearchGate

See discussions, stats, and author profiles for this publication at: https://www.researchgate.net/publication/336993249

In-situ, microscale characterization of heterogeneous deformation around notch in martensitic Shape Memory Alloy

Article *in* Materials Science and Engineering A · November 2019

DOI: 10.1016/j.msea.2019.138605

CITATIONS
0

READS
35

5 authors, including:

Partha Paul
Stanford University
12 PUBLICATIONS **45** CITATIONS
SEE PROFILE

Harshad Paranjape
Nitinol Devices & Components, Inc.
23 PUBLICATIONS **138** CITATIONS
SEE PROFILE

Nobumichi Tamura
Lawrence Berkeley National Laboratory
369 PUBLICATIONS **6,393** CITATIONS
SEE PROFILE

Some of the authors of this publication are also working on these related projects:

Development and application of synchrotron based diffraction techniques; Microstructure-mechanical property relations of metallic materials View project

Electromigration View project

All content following this page was uploaded by Partha Paul on 11 November 2019.

The user has requested enhancement of the downloaded file.

Materials Science & Engineering A xxx (xxxx) xxx

Contents lists available at ScienceDirect

Materials Science & Engineering A

journal homepage: http://www.elsevier.com/locate/msea

Short communication

In-situ, microscale characterization of heterogeneous deformation around notch in martensitic Shape Memory Alloy

Partha P. Paul [a,*], Harshad M. Paranjape [b], Nobumichi Tamura [c], Yuri I. Chumlyakov [d], L. Catherine Brinson [e]

[a] Mechanical Engineering, Northwestern University, Evanston, IL, 60201, USA
[b] Mechanical Engineering, Colorado School of Mines, Golden, CO, 80401, USA
[c] Advanced Light Source, Lawrence Berkeley National Laboratory, Berkeley, CA, 94720, USA
[d] Siberian Physical Technical Institute, Tomsk, 634050, Russia
[e] Mechanical Engineering and Materials Science, Duke University, Durham, NC, 27708, USA

ARTICLE INFO

Keywords:
Nickel Titanium
Shape Memory Alloys
Martensite deformation
Microdiffraction
Notch deformation

ABSTRACT

Deformation characterization of low-symmetry phases such as martensite in SMAs is challenging due to a fine-scale hierarchical microstructure. Using X-ray microLaue diffraction, in-situ deformation of martensite is examined in a notched NiTi specimen. The local deformation is influenced by the notch stress field, initial martensite microstructure, and interaction between notch stress field and the external load. The microstructure evolves heterogeneously and inelastically, with detwinning and twin nucleation occurring simultaneously through loading. These results contrast with the traditional view of martensite deformation that is partitioned in three distinct regimes: elasticity, reorientation and de-twinning.

1. Introduction

Nickel Titanium (NiTi) is commercially the most common Shape Memory Alloy (SMA), widely used in the biomedical field [1]. NiTi undergoes phase transformation between a high crystal symmetry cubic (B2, austenite) and a low crystal symmetry monoclinic (B19', martensite), which has been well studied [2]. Additionally, deformation in the high symmetry austenite phase is well understood [3]. However, due to the challenges associated with its characterization, the deformation mechanics of the low-symmetry martensite phase has received relatively less attention. Martensite in NiTi typically exhibits a hierarchical microstructure [4], from pairs of crystallographic variants (CV) forming twins at the nanoscale to multiple domains of twinned CVs spanning a bulk specimen. Deformation under an external stress in the martensite phase primarily proceeds inelastically through nucleation of new CVs or reorientation of one CV into another [5]. However, the small size of twinned CVs, low crystallographic symmetry, and low activation stress for inelastic deformation makes the characterization of martensite deformation using traditional techniques such as electron microscopy challenging in bulk specimens.

At the nanoscale, transmission electron microscopy (TEM) has been used to study martensite microstructures [6]. However, apart from such techniques being destructive and involving cumbersome sample preparation, the measurements may not be representative of bulk samples, and making in-situ measurements remains challenging. Towards the other end of the spectrum, non destructive bulk techniques like neutron diffraction have been used to study martensite deformation at the specimen-scale [7]. However, such techniques furnish averaged deformation information over thousands of twinned martensite domains and thus are not suitable for studying micro-scale deformation heterogeneity. Thus, there is an opportunity to characterize the heterogeneity in martensite deformation at the microscale, to connect that information to microstructure-scale and specimen-scale phenomena. We choose to pursue this multiscale investigation using notched NiTi specimens, which provide a stress concentration around which heterogeneous martensite deformation can occur.

X-ray-based techniques have been used to characterize deformation primarily in the austenite phase in NiTi [8,9]. While such techniques have also been expanded to characterize deformation in the martensite phase [10] recently, the emphasis has been on uniform samples without any external stress-concentrators. At the microscale, X-ray microLaue diffraction has been used for in-situ characterization of the

* Corresponding author.
E-mail address: parthapaul2018@u.northwestern.edu (P.P. Paul).

https://doi.org/10.1016/j.msea.2019.138605
Received 27 July 2019; Received in revised form 23 September 2019; Accepted 26 October 2019
Available online 1 November 2019
0921-5093/© 2019 Elsevier B.V. All rights reserved.

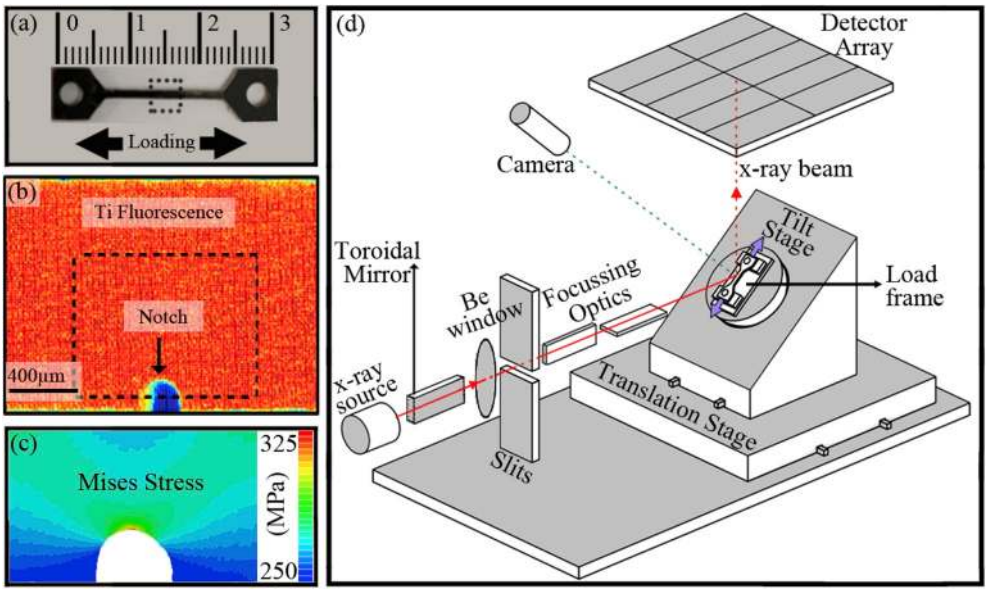

Fig. 1. (a) Dimensions of the specimen used in the tensile experiments. (b) A representative Ti fluorescence scan around the notch at the center of the specimen in (a) indicated by the dotted box. (c) Linear elastic simulation of the Mises stress contour around the notch in the dotted box indicated in (b). (d) Schematic of the load frame in the microLaue beam (adapted from Ref. [14]).

crystallography of martensite in SMAs [11]. This work aims to benefit from the micron-scale spatial resolution of microLaue diffraction and the ability to perform in-situ measurements non-destructively. The goal of this work is to characterize the deformation in a martensitic NiTi specimen with a machined notch and connect the observations to two phenomena: the stress-heterogeneity generated by the notch and the inherent inelastic and anisotropic nature of deformation in martensite phase. Our past work on phase transformation in NiTi specimens with micron-scale holes has demonstrated that the deformation heterogeneity is determined by the interaction between geometrical features of the specimen and microstructural features inherent to the underlying material [12,13] and we expect similar interaction in the martensitic specimens.

2. Materials and methods

The transformation temperatures of the Ni-49.8 at.%-Ti material, as measured using Differential Scanning Calorimetry(DSC) are: $Mf = \approx$ -3 °C, $As = \approx 31$ °C and $Af = \approx 45$ °C, meaning the material is completely martensitic below ≈ -3 °C. The material was grown as an austenite single crystal ingot at ≈ 400 °C using Bridgman technique and cooled down to room temperature. A 1.43 mm thick dogbone sample (Fig. 1 (a)) was machined from the single crystal ingot and loaded to 6% tensile strain, in order to coarsen the size of martensite CVs through twin reorientation. A notch was then machined in one edge of the sample gage (Fig. 1(b)). The specimen surface was then ground and polished (1 μm diamond-based solution; vibratory polishing with 60 nm colloidal silica). Finally, the specimen was dipped in liquid nitrogen for ≈1000s, to ensure the material is martensitic at room temperature. A 3D model was generated using an image of the surface obtained from SEM of the as-machined specimen and a simulation of uniaxial tensile axial loading was performed using an isotropic elastic constitutive law. The goal of this simulation was to isolate the stress asymmetry around the notch (see Fig. 1(c)) purely due to any imperfections in the notch orientation. Note that even though the notch is machined perpendicular to the specimen edge, some imperfections can be present in the notch geometry.

In-situ fluorescence and microLaue diffraction measurements were performed at beamline 12.3.2 at the Advanced Light Source at the Lawrence Berkeley National Laboratory. Fluorescence scans furnish the location of the notch root and also reveal any non-metallic inclusions (e.g., TiC particles) that can potentially alter the local deformation state. MicroLaue diffraction are used to obtain martensite orientations from the specimen surface. A polychromatic X-ray beam (6–24 keV) was focused using Kirkpatrick-Baez mirrors to a 2 μm × 2 μm beam cross-section. A schematic of the experimental setup is shown in Fig. 1(d). The detailed version can be found elsewhere [14]. The diffraction

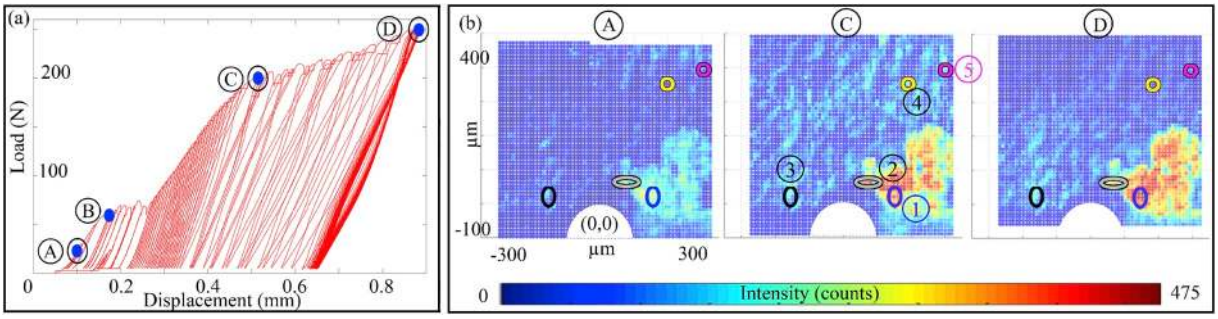

Fig. 2. (a) The nominal load-displacement curve. Loading was interrupted at 15 N,55 N, 200 N and 250 N to obtain diffraction scans. (b) The spatial distribution of the average diffraction intensity (signal to noise ratio) at three of the four load steps. These plots span the area indicated by the dotted box in Fig. 1(b). The five numbered areas, marked by colored ellipses are analyzed in further detail in Fig. 3. (For interpretation of the references to colour in this figure legend, the reader is referred to the web version of this article.)

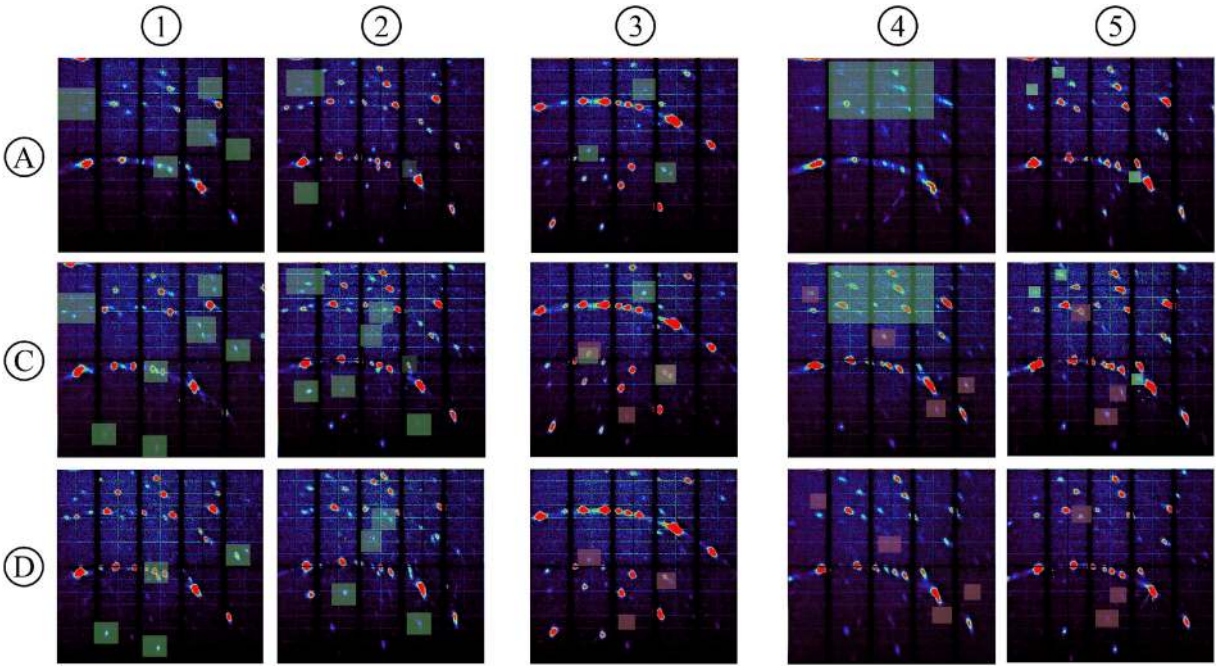

Fig. 3. Evolution of diffraction patterns with loading at the five numbered locations at loading steps Ⓐ, Ⓒ and Ⓓ, as shown in Fig. 2(b). Columns ① and ② lie to the top right of the notch, in the region of high average deformation intensity. The central column (③) lies to the top left of the notch. Columns ④ and ⑤ indicate regions relatively far away from the notch, to the top right of the diffraction area. Green boxes indicate appearance of new spots while purple boxes highlight the disappearance of existing spots. (For interpretation of the references to color in this figure legend, the reader is referred to the Web version of this article.)

patterns were recorded using a DECTRIS Pilatus 1 M area detector placed at a vertical distance of 150.34 mm from the specimen center. A Silicon standard was used to calibrate the sample to detector distance and detector tilts, as described in Ref. [11]. An exposure of 5s was used to record diffraction patterns from the specimen surface around notch in raster mode, with a step size of 10 μm. The diffraction analysis was performed using XMAS software [15].

3. Results and discussion

Uniaxial cyclic tensile loading was performed at room temperature using a Deben dual leadscrew load frame under displacement control at 0.2 mm/min (Fig. 2(a)). Cyclic loading was performed using 5 N increasing load amplitudes, to avoid sudden fracture of the specimen. At Ⓐ: 15 N, Ⓑ: 55 N, Ⓒ: 200 N and Ⓓ: 250 N loads, diffraction data was collected by holding the load, indicated by the blue dots in Fig. 2 (a). These points were selected where the overall load-displacement curve changed slope. Since Ⓑ is at a very low load (≈ 35 N), the deformation between Ⓐ and Ⓑ is expected to be mainly elastic. Therefore, to focus on the inelastic deformation, points Ⓒ and Ⓓ are compared to Ⓐ.

Fig. 2(b) shows spatial plots of the average diffraction pattern intensity at load steps Ⓐ, Ⓒ and Ⓓ. Note that these spatial plots are obtained by rastering the X-ray beam in the area shown by the dotted box in Fig. 1(b). At each spatial point, the background noise is subtracted from the signal and the *average intensity* on the detector calculated and normalized by the incident beam intensity. This *average intensity* indicates the signal to noise ratio. The background-subtracted signal on the detector at each spatial point appears as shown in Fig. 2. A point with a lower *average intensity* is likely to have a microstructure with a multitude of relatively small twinned CVs, resulting in less intense spots on the detector. On the other hand, a point with higher *average intensity* is likely to have fewer but large twinned CV domains resulting in fewer, more intense spots.

This *average intensity* map indicates two regions: (1) a bright region immediately to the top right of the notch, that continuously intensifies with increasing load; and (2) the complementary area outside the bright cloud, where the intensity increases from 15 N to 200 N but decreases at 250 N. The simulated Mises stress in Fig. 1(c) indicates a symmetric stress concentration about the notch. Thus, this observed asymmetric deformation around the notch points towards a microstructural origin. Therefore, to study the inelastic deformation around the notch in further detail, five representative areas situated differently with respect to the notch are chosen as shown by ellipses ① - ⑤ in Fig. 2(b) and the evolution of the diffraction pattern from these five spatial regions is qualitatively compared.

The evolution of the diffraction patterns with loading from areas ① - ⑤ in Fig. 2(b) is shown in Fig. 3. To highlight this evolution of spots in the diffraction pattern, the following color coding is used. At any particular load step, green translucent boxes indicate the appearance of new spots while purple translucent boxes highlight the disappearance of spots that existed at the previous load step. These appearances of new spots in the raw diffraction pattern can be correlated to the deformation mechanisms in martensitic NiTi [8,16]. In terms of the martensite deformation mechanisms, the changes indicated by the green boxes, where new spots appear on loading, are explained by the growth of preferred martensite CVs. This change occurs either by nucleation of a new preferred CV or by existing fine CV twin structure reorienting into a larger single-preferred CV. When a new CV is nucleated, new spots are produced in the diffraction pattern. When a fine twin structure of CVs is present, it typically produces a low-intensity, diffuse signal in the diffraction pattern that is not detectable above noise in the diffraction data. When such fine twins reorient into a single preferred CV, a stronger signal now produces distinct diffraction spots that are detectable above noise levels. Complementarily, the disappearance of spots within the purple boxes indicates that the martensite CV that originally produced that spot reoriented through the mechanism of twin reorientation, thus causing existing diffraction spot associated with that CV to disappear.

New spots appear (green boxes) at all three loading steps in Areas ① and ②. These regions are situated at the edge and center of the high intensity region shown in Fig. 2(b) and indicate nucleation of new CVs or

spatial coalescence of small domains into larger domains with loading. This observation can be understood as follows. Since the specimen was pre-deformed prior to the diffraction measurements, certain martensite CVs as favored by the uniaxial pre-load were present in the specimen. The stress state around the notch is multi-axial. Thus, at loads Ⓐ, Ⓒ and Ⓓ, new martensite CVs that are favored by the multi-axial stress state would have formed through nucleation or reorientation of existing variants, causing appearance of new diffraction spots. Its is notable that area ③, which is likely to encounter similar stress states as areas ① and ②, did not exhibit appearance of new spots. This difference may have to do with the starting CV distribution in ③, since the spot pattern in ③ is significantly different than ① and ② at a low load. In summary, the diffraction pattern evolution in regions ① - ③ can be rationalized on the basis of formation of new CVs favored by the multi-axial stress state near the notch, with the spatial heterogeneity between these points likely determined by the initial microstructure.

In regions ④ and ⑤ that are far away from the notch, some new spots appear at loading steps Ⓐ and Ⓒ, followed by disappearance of spots in loading step Ⓓ. This observation can be understood as follows. During lower external load at Ⓐ and Ⓒ, new variants formed due to the multi-axial stress field of the notch and thus new diffraction spots appeared. However, at higher loads, the axial loading likely dominated over the stress field of the notch. Thus, a new stress state formed in regions ④ and ⑤, leading to the disappearance of some of the spots. In summary, the deformation in regions ④ and ⑤ is likely to be the result of interaction between the stress field of the notch and the far-field applied axial load.

These results indicate the influence of three factors on the deformation evolution: stress concentration at the notch (Areas ①, ②), initial martensite microstructure (Area ③), and interaction between the far-field load and the stress field around the notch (Areas ④, ⑤). It is known that the martensite microstructure around notches can be different compared to that in homogeneous specimens under uniaxial loading [17] and that after a load path change, martensite CVs can reorient to respond to the new load [18]. Homogeneous martensitic samples tend to form localized Luders-type deformation bands at high external loads [8,10]. Such is not the case with stress concentrators, likely because the stress concentration itself provides an opportunity for deformation localization. A notable observation here is that martensite CV nucleation and reorientation can occur in specimens with stress concentrators starting at very low external loads. This is in contrast with the traditional classification of the martensitic stress-strain response in three distinct regimes: elastic, CV reorientation, and de-twinning of CV twin domains. Thus NiTi parts with porous structures can exhibit inelastic deformation at relatively small loads in the martensite phase and microstructurally sensitive, inelastic deformation models may be essential in simulating their response.

Finally, this work demonstrates that in-situ microLaue diffraction provides a reasonable balance between characterizing a bulk specimen while still capturing microstructural deformation mechanisms. The microstructural detail of this method is superior to neutron diffraction [7] or digital image correlation studies [19] and comparable to recent high-energy X-ray diffraction work [20]. The interrogated area is significantly larger than TEM-based observations of martensite deformation [21]. However, the low crystal symmetry and hierarchical microstructure of the martensite phase renders the quantification of deformation via calculation of lattice strains in microLaue diffraction quite challenging.

Acknowledgements

Financial support for this work was provided by the Department of Energy (DOE), Office of Basic Energy Science (BES), under grant no. DE-SC0010594. The MatCI (NSF DMR-1121262) facility at Northwestern University was used for calorimetry. The authors thank Dr. Camelia Stan (ALS) for help with diffraction experiments, and Prof. A. Stebner and Dr. Marc Palmeri for critiquing this manuscript. The microLaue experiments and data analysis were conducted at the Advanced Light Source and National Energy Research Scientific Computing Center respectively, supported by DOE(BES), under DE-AC02-05CH11231.

References

[1] A. Bansiddhi, T. Sargeant, S. Stupp, D. Dunand, Porous niti for bone implants: a review, Acta Biomater. 4 (2008) 773–782.
[2] A.W. Richards, R.A. Lebensohn, K. Bhattacharya, Interplay of martensitic phase transformation and plastic slip in polycrystals, Acta Mater. 61 (2013) 4384–4397.
[3] H.M. Paranjape, P.P. Paul, H. Sharma, P. Kenesei, J.-S. Park, T. Duerig, L. C. Brinson, A.P. Stebner, Influences of granular constraints and surface effects on the heterogeneity of elastic, superelastic, and plastic responses of polycrystalline shape memory alloys, J. Mech. Phys. Solids 102 (2017) 46–66.
[4] K. Bhattacharya, Microstructure of Martensite: Why it Forms and How it Gives Rise to the Shape-Memory Effect, Oxford University Press, 2003.
[5] P. Mullner, A. King, Deformation of hierarchically twinned martensite, Acta Mater. 58 (2010) 5242–5261.
[6] W. Gao, X. Yi, B. Sun, X. Meng, W. Cai, L. Zhao, Microstructural evolution of martensite during deformation in zr50cu50 shape memory alloy, Acta Mater. 132 (2017) 405–415.
[7] R. Vaidyanathan, M.A.M. Bourke, D.C. Dunand, Texture, strain, and phase-fraction measurements during mechanical cycling in superelastic NiTi, Metall. Mater. Trans. A 32 (2001) 777–786.
[8] H.M. Paranjape, P.P. Paul, B. Amin-Ahmadi, H. Sharma, D. Dale, J.P. Ko, Y. I. Chumlyakov, L.C. Brinson, A.P. Stebner, In situ, 3d characterization of the deformation mechanics of a superelastic niti shape memory alloy single crystal under multiscale constraint, Acta Mater. 144 (2018) 748–757.
[9] S.W. Robertson, A. Mehta, A.R. Pelton, R.O. Ritchie, Evolution of crack-tip transformation zones in superelastic Nitinol subjected to in situ fatigue: a fracture mechanics and synchrotron X-ray microdiffraction analysis, Acta Mater. 55 (2007) 6198–6207, 18 bibtex: Robertson2007.
[10] A.N. Bucsek, D.C. Pagan, L. Casalena, Y. Chumlyakov, M.J. Mills, A.P. Stebner, Ferroelastic twin reorientation mechanisms in shape memory alloys elucidated with 3d x-ray microscopy, J. Mech. Phys. Solids 124 (2019) 897–928.
[11] X. Chen, C. Dejoie, T. Jiang, C.-S. Ku, N. Tamura, Quantitative microstructural imaging by scanning laue x-ray micro-and nanodiffraction, MRS Bull. 41 (2016) 445–453.
[12] P.P. Paul, H.M. Paranjape, B. Amin-Ahmadi, A.P. Stebner, D.C. Dunand, L. C. Brinson, Effect of machined feature size relative to the microstructural size on the superelastic performance in polycrystalline niti shape memory alloys, Mater. Sci. Eng. A 706 (2017) 227–235.
[13] P.P. Paul, M. Fortman, H.M. Paranjape, P.M. Anderson, A.P. Stebner, L.C. Brinson, Influence of Structure and Microstructure on Deformation Localization and Crack Growth in Niti Shape Memory Alloys, Shape Memory and Superelasticity, 2018.
[14] N. Tamura, M. Kunz, K. Chen, R. Celestre, A. MacDowell, T. Warwick, A superbend x-ray microdiffraction beamline at the advanced light source, Mater. Sci. Eng. A 524 (2009) 28–32.
[15] N. Tamura, XMAS: A Versatile Tool for Analyzing Synchrotron X-Ray Microdiffraction Data, Imperial College Press, 2014, pp. 125–155.
[16] A.N. Bucsek, D. Dale, J.Y.P. Ko, Y. Chumlyakov, A.P. Stebner, Measuring stress-induced martensite microstructures using far-field high-energy diffraction microscopy, Acta Crystallogr. A: Found. Adv. 74 (2018).
[17] T. Niendorf, P. Krooß, C. Somsen, G. Eggeler, Y.I. Chumlyakov, H.J. Maier, Martensite aging – avenue to new high temperature shape memory alloys, Acta Mater. 89 (2015) 298–304.
[18] W.-N. Hsu, E. Polatidis, M. Šmíd, N. Casati, S. Van Petegem, H. Van Swygenhoven, Load path change on superelastic niti alloys: in situ synchrotron xrd and sem dic, Acta Mater. 144 (2018) 874–883.
[19] G. Laplanche, T. Birk, S. Schneider, J. Frenzel, G. Eggeler, Effect of temperature and texture on the reorientation of martensite variants in niti shape memory alloys, Acta Mater. 127 (2017) 143–152.
[20] P. Sedmák, J. Pilch, L. Heller, J. Kopeček, J. Wright, P. Sedlák, M. Frost, P. Šittner, Grain-resolved analysis of localized deformation in nickel-titanium wire under tensile load, Science 353 (2016) 559–562.
[21] W. Gao, X. Yi, B. Sun, X. Meng, W. Cai, L. Zhao, Microstructural evolution of martensite during deformation in zr50cu50 shape memory alloy, Acta Mater. 132 (2017) 405–415.

View publication stats